Sparse Metasurfaces: From Theory to Practical Implementations

Vladislav Popov, Thomas Lepetit, Fabrice Boust, Shah Nawaz Burokur

Sparse Metasurfaces: From Theory to Practical Implementations

Vladislav Popov[1], Thomas Lepetit[2], Fabrice Boust[2], Shah Nawaz Burokur[3]
[1] SONDRA, CentraleSupélec, Université Paris-Saclay, F-91190, Gif-sur-Yvette, France
[2] DEMR, ONERA, Université Paris-Saclay, F-91123, Palaiseau, France, thomas.lepetit@onera.fr
[3] LEME, UPL, Univ Paris Nanterre, F-92410, Ville d'Avray, France, sburokur@parisnanterre.fr

***Abstract*—Metagratings demonstrate an exceptional efficiency in controlling diffraction patterns. Still, they are essentially periodic structures excited by a plane wave. This induces two main drawbacks. First, periodicity limits metagratings to the control of a discrete set of scattered plane waves, not a continuous one. Second, plane-wave-like illumination assumes that the source is placed in the far-field, significantly reducing feeding efficiency. Here, we elaborate on the analytical model of metagratings and show how numerical calculation of Green's functions can be employed to overcome these drawbacks and design *sparse metasurfaces* capable of creating arbitrary radiation patterns for arbitrary external excitations.**

***Index Terms*—*sparse metasurfaces, Green's function, load impedance,*.**

I. INTRODUCTION

In the last two decades, metasurfaces, thin two-dimensional metamaterials, have proven themselves as a powerful tool to tailor wavefronts [1]. By controlling their reflection and/or transmission characteristics, metasurfaces have been successfully implemented in antennas [2], lenses [3], anomalous reflection and refraction devices [4-7], polarization converters [8], vortex beam generators [9-10] and holograms [11-12]. For wavefront manipulation, most metasurfaces rely on the generalized law of reflection and refraction discussed in [4] and such classical metasurfaces are composed of densely packed meta-atoms with local electromagnetic responses. However, several studies have shown that this approach suffers from low efficiency, particularly in configurations where extreme wave manipulation is considered [13-15].

Recently, metagratings have been proposed as an interesting alternative to metasurfaces for enhancing wavefront manipulation efficiency [16-23]. They are designed to engineer diffraction by cancelling a finite number of undesired propagating diffraction orders and allowing desired ones to radiate. In general, a metagrating is an array of scatterers separated by a distance of the order of the operating wavelength. Compared to metasurfaces, the sparse arrangement of scatterers does not allow a description of metagratings in terms of local reflection and transmission coefficients (or surface impedances). A metagrating consists of a limited number of meta-atoms in a supercell (period) compared to a metasurface that is composed of supercells incorporating numerous meta-atoms with subwavelength periodicity.

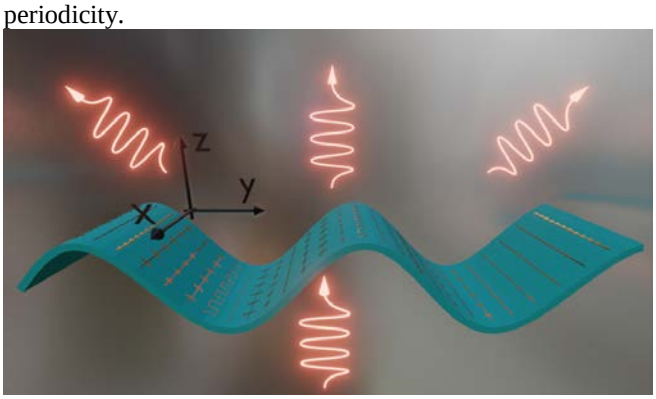

Fig. 1. Schematic of the proposed approach. An arbitrarily shaped sparse metasurface is designed to transform an illuminating excitation into any desired radiation configuration.

Although metagratings demonstrate an exceptional efficiency in controlling diffraction patterns, they are essentially periodic structures excited by a plane wave. The periodicity makes the functionality of metagratings limited to control a discrete set of scattered plane waves. Furthermore, a plane-wave-like illumination reduces considerably the range of applications. Actually, there is no reason that a set of scatterers can only reflect a wave on a discrete set of directions. These limitations come from the mathematical approach used, which is based on the periodicity.

In this work, we have consequently developed an original approach, which can be employed to design arbitrarily shaped sparse metasurfaces, capable of creating almost any desired radiation patterns for any type of external excitation. The paper is organized as follows. In Section II, after detailing the definition of a *sparse metasurface*, we describe the theory and the established methodology enabling to design the latter sparse metasurface. In Section III, an implementation example is presented to illustrate the merits of the proposed approach. Finally, Section IV provides some discussions on the pros and cons of the approach.

II. THEORY AND METHODOLOGY

A sparse metasurface is composed of a finite set of N arbitrarily distributed loaded parallel wires. Microscopically, a loaded wire represents itself as a chain of subwavelength meta-atoms. On the other hand, macroscopically, we model the loaded wire as uniform with an effective linear

impedance density and having a deeply subwavelength effective radius r_{eff}. The main differences with a metagrating are:

- Sparse metasurfaces are non-periodic and the number of wires is finite,
- The wires are not necessarily arranged on a planar surface,
- The external excitation does not need to be a plane-wave illumination and can be any arbitrary complex wave configuration.

In the following, we assume that the translation symmetry is along the *x*-axis. Electric field directed along *x*-axis of a background wave radiated by an external source excites polarization currents in the loaded wires. The polarization currents I_q, excited in the wires can shape the field radiated by the sparse metasurface in accordance with the following equation [24]:

$$E_x(r,\varphi) = E_x^{(ext)}(r,\varphi) + \sum_{q=1}^{N} G_{xx}(r,\varphi;\mathbf{r}_q) I_q \qquad (1)$$

where r and φ are polar coordinates. The total field $E_x(r,\varphi)$ is represented by the superposition of the wave radiated by the external sources $E_x^{(ext)}(r,\varphi)$ and waves $G_{xx}(r,\varphi;\mathbf{r}_q)I_q$ scattered by the wires, with $G_{xx}(r,\varphi;\mathbf{r}_q)$ being a Green's function corresponding to the q^{th} wire at $\mathbf{r}_q$. Importantly, $E_x^{(ext)}$ and Green's functions should be calculated in the presence of the substrate and all other non-engineered elements of the sparse metasurface, such as for *e.g.*, the substrate supporting external sources.

The suitable currents I_q can be obtained by loading the wires with suitable load-impedance densities Z_q, which are related by the Ohm's law:

$$Z_q I_q = E_x^{(ext)}(\mathbf{r}_q) - \sum_{p=1}^{N} Z_{qp} I_p \qquad (2)$$

A load-impedance density Z_q is a characteristic of a loaded wire and can be engineered for instance by tuning the geometrical parameters of the meta-atoms [23-24] or with the help of tunable elements such as varactor diodes [25]. The right-hand side of Eq. (2) represents the total electric field at the position of the q^{th} wire, where

$$Z_{qp} = -G_{xx}(\mathbf{r}_q,\mathbf{r}_p) \qquad (3)$$

is the mutual-impedance density (the electric field created by the p^{th} wire, with a current of 1A, at the position of the q^{th} wire). The separation between two neighboring wires can be arbitrary as long as polarization currents in wires can be approximated by a 2D delta function. As it is demonstrated further, this simple model works surprisingly well even for complex designs. The self-action of the q^{th} wire and its interaction with a substrate and an environment is accounted via the formula:

$$Z_{qq} = \frac{-1}{2\pi r_{eff}} \oint G_{xx}(\mathbf{r};\mathbf{r}_q)\mathrm{d}\mathbf{r} \qquad (4)$$

where the integration is performed over the circumference of the wire of effective radius r_{eff}.

The question is about the choice of the value of N and the consequences of this choice on the required Z_q to construct the desired field configuration. Each term on the right-hand side of Eq. (1) at a given distance r can be approximated by a partial Fourier sum over the polar angle φ: $E_x^{(ext)}(r,\varphi) = \sum_{-M}^{M} C_n^{(ext)} e^{in\varphi}$ and $G_{xx}(r,\varphi;\mathbf{r}_q) = \sum_{-M}^{M} C_n^{(q)} e^{in\varphi}$. M is the maximum Fourier harmonic defined as the minimum number M such that

$$\left|C_{\pm|M+r|}^{(ext,q)}\right| / \max\left|C_n^{(ext,q)}\right| \ll 1 \qquad (5)$$

for all r = 1, 2, … Many parameters might affect M but the most important one is the physical aperture of the metasurface. The larger the aperture the greater is M. The total electric field $E_x(r,\varphi)$ can also be represented by a partial Fourier sum $\sum_{-M}^{M} C_n e^{in\varphi}$ which, using Eq. (1), gives a relation between the Fourier coefficients:

$$C_n = E_n^{(ext)} + \sum_{q=1}^{N} C_n^{(q)} I_q \qquad (6)$$

When a sparse metasurface is composed of at least $N = 2M + 1$ loaded wires, one can establish arbitrary azimuthal field distributions within the functional space of the $2M + 1$ Fourier harmonics by adopting the Fourier coefficients C_n. Corresponding load-impedance densities can be found from Eq. (2) after solving Eq. (6) with respect to I_q, which in this case has a single solution. As a matter of fact, there is no guarantee that the analytically found Z_q would not require implementing active and/or lossy elements. Additionally, in order to only deal with reactive load-impedance densities, one might need a number of wires $N \geq 2M + 1$ to construct arbitrary radiation patterns, as recently discussed in Ref. [21].

The choice of the number of loaded wires N is a major point and may require several iterations. Indeed, to achieve, for instance, beamforming in one direction, it might not be required to control all $2M + 1$ of the Fourier harmonics and therefore, a smaller number of wires can be used. On the other hand, prohibiting active elements tends to increase N. Lastly, not all reactive load-impedance densities can be synthesized. In practice, after selecting the N value, an optimization algorithm is applied to obtain the load-impedance densities solving Eqs. (1) and (2) with constraints on the real and imaginary parts of Z_q. For instance, the following objective function can be used to construct a single beam at the angle φ^* and minimize the level of side-lobes:

$$f(\{Z_q\}) = 20\log_{10}\left[\left|E_{ff}(\varphi^*)\right| / \max_{\varphi}\left|E_{ff}(\varphi)\right|\right] \qquad (7)$$

where $E_{ff}(\varphi)$ is the total electric field in the far-field region and the function $\max_{\varphi}$ finds the maximum among discrete values of $E_{ff}(\varphi)$. The maximum of $\left|E_{ff}(\varphi)\right|$ is searched in all directions of a discretized far-field pattern except from the

range of angles corresponding to the desired beam. The optimization parameters are the geometrical parameters of meta-atoms composing the wires and the number of wires.

Once the Z_q are calculated, the design of loaded wires is performed within the local periodic approximation (LPA), developed in Ref. [22]. It may be possible to obtain an analytical model linking load impedance densities and some geometrical parameters. In these conditions, the optimizing procedure can directly establish the suitable set of geometrical parameters. A particular importance of the LPA of Ref. [22] should be emphasized: Sparse metasurfaces cannot be designed as their dense counterparts. Indeed, the design procedure results in the load-impedance density of a loaded wire, which is its proper characteristic and depends on neither the substrate's thickness nor the inter-wire distance [23]. On the other hand, when designing conventional dense metasurfaces, one deals with such characteristics as surface impedances (or local reflection and/or transmission coefficients), which represent the integral response a unit cell and depend on the parameters of a substrate and the inter-element distance.

III. Implementation Example

In this example, we consider a planar sparse metasurface placed on the top of an open rectangular PEC cavity excited by a coaxial probe, as illustrated in Fig. 2. Fig. 3 shows the distribution of the excitation field created by the probe and an example of function $G_{xx}(\mathbf{r};\mathbf{r}_q)$ calculated for this configuration at an operation frequency of 10 GHz.

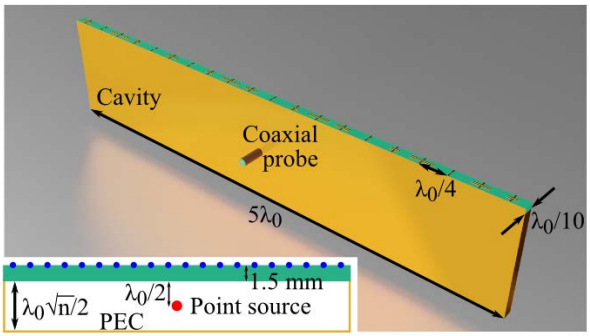

Fig. 2. 3D schematics of cavity-excited flat sparse metasurface having 20 wires. The dielectric substrate used is 1.5 mm thick F4BM220, the cavity height is $\frac{\lambda_0\sqrt{n}}{2} \approx 33.5$ mm, where n is the cavity length ($5\lambda_0$) divided by the wavelength λ_0. Operating frequency is set to 10 GHz.

For the given aperture size of $5\lambda_0$, the number $2M + 1$ of independent Fourier harmonics forming the far-field pattern equals 42. The optimization procedure, where the continuous function of the electric field is discretized, has been applied for 10 ($\lambda_0/2$ inter-wire distance) and 20 ($\lambda_0/4$ inter-wire distance) loaded wires. The discretization is as fine as it is necessary to take into account all side lobes. While neither 10 nor 20 wires is enough to arbitrarily control 42 Fourier harmonics, it is however possible to perform efficient beam forming.

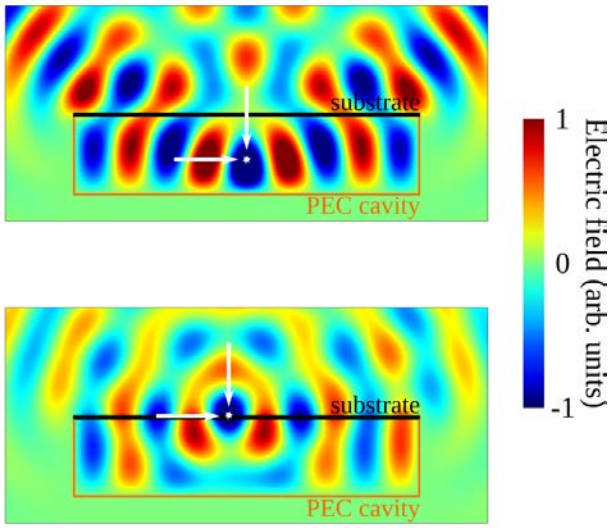

Fig. 3. Simulated distributions of the electric field created by an elementary source in different cnfigurations for the open Fabry-Perot cavity covered with a planar dielectric substrate: (Top) excitation field with external elementary source shown by arrows, and (Bottom) function $G_{xx}(\mathbf{r};\mathbf{r}_q)$ obtained as the electric field radiated by an elementary source located at $\mathbf{r}_q$ illustrated by arrows.

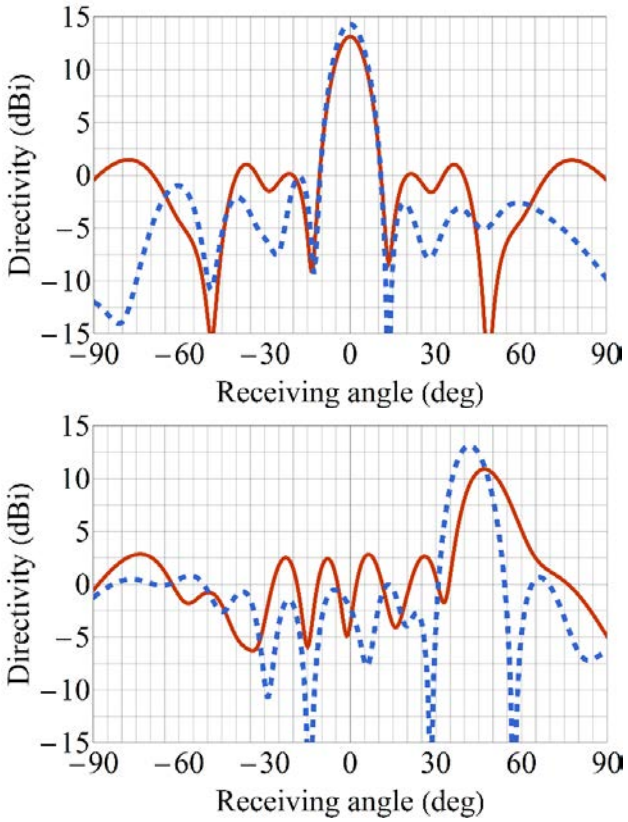

Fig. 4. Comparison of 3D full-wave simulation results for two far-field patterns configuration; boresight beam and 45° steered beam. For each configuration, 10 (red traces) and 20 (blue dotted lines) loaded wires are implemented. or metasurfaces with 10 and 20 wires. The Z_q are succesfully optimized for a radiation at broaside direction (top) and at 45° (bottom).

3D full wave simulations results for two different far-field configurations with 10 and 20 loaded wires are compared in Fig. 4. The two desired far-field patterns are a boresight beam and a 45° steered beam. The comparison between the use of 10 wires (red solid lines) and 20 wires (blue dotted lines) reveals an important result; two times more wires lead to a maximum of only 2 dBi improvement of the directivity. Therefore, one should carefully choose the number of wires as comparable performances can be achieved with a lesser effort, which can be particularly advantageous for reconfigurable designs.

In summary, the presented analytical model allows one to optimize the number of elements by considering a beforehand computed Green's function and without involving time-consuming 3D full-wave simulations of real designs.

IV. Conclusion and Discussion

The method presented in this work applies to structures derived from metagratings, but overcomes their limitations. Indeed, it has the potential to treat sets of parallel wires, without any periodicity and distributed over non-planar arbitrarily shaped surfaces. The approach is based on the numerical calculation of Green's functions for the structure that accommodates the set of wires and of each wire placed in the latter structure. It therefore consists in choosing a number of wires and achieving, with the help of an optimization algorithm, for a set of linear impedance densities, a radiated field that best fits the desired goal.

Interestingly, the implementation example illustrated in Section III suggests that optimization can lead to a number of wires that is less than the independent Fourier harmonics forming the far-field pattern. Performances equivalent or superior to those of traditional metasurfaces but with a smaller number of elements can thus be obtained. This contributes to the reduction of losses and simplifying the implementation, in particular for reconfigurable metasurfaces.

Currently, this approach only deals with 2D configurations and it is natural to wonder about the possibility of a generalization to 3D configurations. It seems possible to transpose the approach by no longer considering sets of wires but sets of meta-atoms whose polarizability would be adjustable. However, the difficulty will be to achieve the required polarizabilities with just one small element. Nevertheless, there are many situations (linearly polarized antennas, cylindrical lenses, polarizer, …) that can be approximated as 2D configurations and in such cases, the methodology will be particularly advantageous.

References

[1] C. L. Holloway, E. F. Kuester, J. A. Gordon, J. O'Hara, J. Booth, and D. R. Smith, "An overview of the theory and applications of metasurfaces: the two-dimensional equivalents of metamaterials," *IEEE Antennas Propag. Mag*., vol. 54, no. 2, pp. 10-35, July 2012.

[2] B. Ratni, W. Merzouk, A. de Lustrac, S. Villers, G.-P. Piau, and S. N. Burokur, "Design of phase-modulated metasurfaces for beam steering in Fabry-Perot cavity antennas," *IEEE Antennas Wireless Propag. Lett.*, vol. 16, pp. 1401-1404, 2017.

[3] K. Zhang, Y. Yuan, X. Ding, B. Ratni, S. N. Burokur, and Q. Wu, "High-efficiency metalenses with switchable functionalities in microwave region," *ACS Appl. Mater. Int*., vol. 11, no. 31, pp. 28423-28430, Aug. 2019.

[4] N. Yu, P. Genevet, M. A. Kats, F. Aieta, J.-P. Tetienne, F. Capasso, and Z. Gaburro, "Light propagation with phase discontinuities: generalized laws of reflection and refraction," *Science*, vol. 334, no. 6054, pp. 333-337, Oct. 2011.

[5] A. Díaz-Rubio, V. S. Asadchy, A. Elsakka, and S. Tretyakov, "From the generalized reflection law to the realization of perfect anomalous reflectors," *Sci. Adv*., vol. 3, no. 8, p. e1602714, Aug. 2017.

[6] B. Ratni, A. de Lustrac, G.-P. Piau, and S. N. Burokur, "Reconfigurable meta-mirror for wavefronts control: applications to microwave antenna," *Opt. Express*, vol. 26, no. 3, pp. 2613-2624, Feb. 2018.

[7] Y. Yuan, K. Zhang, X. Ding, B. Ratni, S. N. Burokur, and Q. Wu, "Complementary transmissive ultra-thin meta-deflectors for broadband polarization-independent refractions in the microwave region," *Photon. Res*., vol. 7, no. 1, pp. 80-88, Jan. 2019.

[8] B. Ratni, A. de Lustrac, G.-P. Piau, and S. N. Burokur, "Electronic control of linear-to-circular polarization conversion using a reconfigurable metasurface," *Appl. Phys. Lett.*, vol. 111, no. 21 p. 214101, Nov. 2017.

[9] M. L. N. Chen, L. J. Jiang, and W. E. I. Sha, "Ultrathin complementary metasurface for orbital angular momentum generation at microwave frequencies," *IEEE Trans. Antennas Propag*., vol. 65, no. 1, pp. 396-400, Jan. 2017.

[10] Y. Yuan, K. Zhang, B. Ratni, Q. Song, X. Ding, Q. Wu, S. N. Burokur, and P. Genevet, "Independent phase modulation for quadruplex polarization channels enabled by chirality-assisted geometric-phase metasurfaces," *Nat. Commun*., vol. 11, no. 1, p. 4186, Aug. 2020.

[11] Z. Wang X. Ding, K. Zhang, B. Ratni, S. N. Burokur, X. Gu, and Q. Wu, "Huygens metasurface holograms with the modulation of focal energy distribution," *Adv. Opt. Mater*., vol. 6, no. 12, p. 1800121, June 2018.

[12] C. Guan, J. Liu, X. Ding, Z. Wang, K. Zhang, H. Li, M. Jin, S. N. Burokur, and Q. Wu, "Dual-polarized multiplexed meta-holograms utilizing coding metasurface," *Nanophotonics*, vol. 9, no. 11, pp. 3605-3613, Sep. 2020.

[13] V. S. Asadchy, M. Albooyeh, S. N. Tcvetkova, A. Díaz-Rubio, Y. Ra'di, and S. A. Tretyakov, "Perfect control of reflection and refraction using spatially dispersive metasurfaces," *Phys. Rev. B*, vol. 94, p. 075142, Aug. 2016.

[14] N. M. Estakhri and A. Alù, "Wave-front transformation with gradient metasurfaces," *Phys. Rev. X*, vol. 6, no. 4, pp. 1–17, 2016.

[15] A. Epstein and G. V. Eleftheriades, "Huygens' metasurfaces via the equivalence principle: design and applications," *J. Opt. Soc. Am. B*, vol. 33, no. 2, pp. A31–A50, Feb 2016.

[16] Y. Ra'di, D. L. Sounas, and A. Alù, "Metagratings: Beyond the limits of graded metasurfaces for wave front control," *Phys. Rev. Lett*., vol. 119, p. 067404, Aug. 2017.

[17] A. Epstein and O. Rabinovich, "Unveiling the properties of metagratings via a detailed analytical model for synthesis and analysis," *Phys. Rev. Appl.*, vol. 8, p. 054037, Nov 2017.

[18] O. Rabinovich and A. Epstein, "Analytical design of printed circuit board (pcb) metagratings for perfect anomalous reflection," *IEEE Trans. Antennas Propag*., vol. 66, no. 8, pp. 4086–4095, Aug. 2018.

[19] O. Rabinovich, I. Kaplon, J. Reis, and A. Epstein, "Experimental demonstration and in-depth investigation of analytically designed anomalous reflection metagratings," *Phys. Rev. B*, vol. 99, p. 125101, March 2019.

[20] V. Popov, F. Boust, and S. N. Burokur, "Controlling diffraction patterns with metagratings," *Phys. Rev. Appl*., vol. 10, p. 011002, July 2018.

[21] V. Popov, F. Boust, and S. N. Burokur, "Constructing the near field and far field with reactive metagratings: Study on the degrees of freedom," *Phys. Rev. Appl*., vol. 11, p. 024074, Feb. 2019.

[22] V. Popov, M. Yakovleva, F. Boust, J.-L. Pelouard, F. Pardo, and S. N. Burokur, “Designing metagratings via local periodic approximation: From microwaves to infrared,” *Phys. Rev. Appl*., vol. 11, no. 4, p. 044054, April 2019.

[23] V. Popov, F. Boust, and S. N. Burokur, “Beamforming with metagratings at microwave frequencies: design procedure and experimental demonstration,” *IEEE Trans. Antennas Propag*., vol. 68, no. 3 (Part1), pp. 1533-1541, March 2020.

[24] V. Popov, S. N. Burokur, and F. Boust, “Conformal sparse metasurfaces for wavefront manipulation,” *Phys. Rev. Appl*., vol. 14, no. 4, p. 044007, Oct. 2020.

[25] V. Popov, B. Ratni, S. N. Burokur, and F. Boust, “Non-local reconfigurable sparse metasurface: Efficient near-field and far-field wavefront manipulations,” *arXiv:2009.11699*, Sep. 2020.